

## Light-scattering study of phonon-magnon coupling in antiferromagnetic $\text{FeCl}_2 \cdot 2\text{H}_2\text{O}$ <sup>†</sup>

R. W. Kinne,\* W. J. O'Sullivan, J. F. Ryan,<sup>‡</sup> and J. F. Scott

Department of Physics, University of Colorado, Boulder, Colorado 80302

(Received 22 July 1974)

Raman spectroscopy has been used to study the phonon-magnon coupling in the antiferromagnetic phase of ferrous chloride dihydrate. The interaction has been studied as a function of temperature, from 2 K to  $T_N = 23$  K, and applied field, from 0 to 28 kG. The phonon is assigned as a  $B_g$  symmetry libration mode, in accord with the predictions of Torrance and Slonczewski; it is found to be "soft," decreasing in energy as  $T \rightarrow 0$ . The phonon-magnon coupling constant is nearly field independent but decreases to zero at  $T_N$ . It is found that no zero-field splitting of the magnon occurs, within  $0.2\text{-cm}^{-1}$  instrumental resolution, in contrast to the  $0.8\text{-cm}^{-1}$  splitting inferred from the infrared spectrum. The magnon  $g$  value is determined to be  $1.7 \pm 0.1$ , in contrast to Torrance's value of  $2.23 \pm 0.02$ .

### I. INTRODUCTION

The interaction of optical and acoustic phonons with spin waves in antiferromagnetic insulators has provided the basis for several theoretical and experimental studies over the past few years.<sup>1-10</sup> The most complete work has been presented by Buyers *et al.* on  $\text{KCoF}_3$ ,<sup>4</sup> and by Torrance and co-workers on the  $\text{FeCl}_2 \cdot 2\text{H}_2\text{O}$  family.<sup>5-7</sup> Recently, we performed a series of Raman experiments on  $\text{FeCl}_2 \cdot 2\text{H}_2\text{O}$  which permit a quantitative analysis of the phonon-magnon coupling.<sup>11</sup> The analysis is based on earlier studies of phonon interactions and yields temperature and field dependences of the coupling constant, as well as a quantitative calculation of lines shapes for the coupled modes.

The class of metal-halide dihydrates with chemical formula  $\text{MX}_2 \cdot 2\text{H}_2\text{O}$ , where  $M$  is a divalent metal ion ( $\text{Fe}^{2+}$ ,  $\text{Co}^{2+}$ ,  $\text{Mn}^{2+}$ ) and  $X$  is a halide ( $\text{Cl}^{1-}$ ,  $\text{Br}^{1-}$ ), has been the subject of much recent investigation. These compounds generally exhibit magnetic behavior,<sup>12,13</sup> with typical ordering temperatures up to  $\sim 23$  K. The dihydrates of iron and cobalt chloride and cobalt bromide show two discontinuous magnetic transitions<sup>12,13</sup> below a triple point  $T_T$ , and are thus of particular interest because of their three stable magnetically ordered phases. Their simple crystal structure makes them attractive for experimental study; they are monoclinic with two identical formula groups in the unit cell. A third feature which makes these crystals a source of important data is the existence of strong exchange fields in their ordered states.<sup>13,14</sup>

### II. STRUCTURE, MAGNETIC, AND OPTICAL PROPERTIES

#### A. Structure

The structures of the above dihydrated salts have been established by Morosin,<sup>15-17</sup> with the exception of the iron bromide. All are isomorphous. The manganese salts have received little attention because of their low transition temperatures ( $\sim 2$  K).

Consequently, experimental studies have concentrated on the iron and cobalt salts, in particular  $\text{FeCl}_2 \cdot 2\text{H}_2\text{O}$  and  $\text{CoCl}_2 \cdot 2\text{H}_2\text{O}$ , which we shall abbreviate as FC2 and CC2 in much of what follows.

The crystal structure of FC2 and CC2 is monoclinic, with space-group symmetry  $C_{2h}^3$  (or  $C2/m$ ), indicating a two-fold rotation axis and a perpendicular mirror plane. The metal and chlorine atoms form linear chains (in the  $ac$  mirror plane) which extend along the  $c$  axis, with planar coordination of the iron atom showing a slight deviation from a square. (See Fig. 1.) The waters of hydration are located along the positive and negative  $b$  axis (the axis of rotation) with the H-O-H bond canted out of the  $ab$  plane. The neighboring chains are held together by weak hydrogen bonding to the chlorine ions, and thus the crystal cleaves easily in any plane containing the  $c$  axis. The unit cell consists of two formula groups or primitive cells, which are equivalent and related through the choice

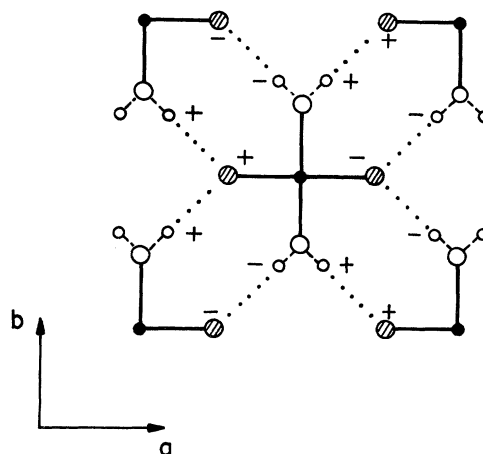


FIG. 1. Structure of  $\text{FeCl}_2 \cdot 2\text{H}_2\text{O}$ . Solid circles: Fe ions; shaded circles: Cl ions; large open circles: oxygen ions; small open circles: protons. + and - signs refer to displacements above and below the  $ab$  plane.

of cell center.

### B. Magnetic properties

Because of the isomorphous nature of CC2 and FC2, one would anticipate closely related magnetic properties. Some difference, however, could be expected. The  $\text{Co}^{2+}$  ion has an odd number of electrons,  $3d^7$ ; consequently, the crystal-field and spin-orbit splitting will leave the ground state as a Kramers doublet.<sup>18</sup> The divalent iron  $\text{Fe}^{2+}$  has a ground-state configuration  $3d^6$ , with the low symmetry leaving the ground state an orbital singlet.

The magnetic properties of FC2 were investigated by Narath.<sup>12</sup> The principal susceptibilities at 76 K were found to be

$$\chi_\alpha = 0.070 \pm 0.002 \text{ emu/mole}, \quad (1a)$$

$$\chi_\beta = 0.040 \pm 0.002 \text{ emu/mole}, \quad (1b)$$

$$\chi_\gamma = 0.041 \pm 0.002 \text{ emu/mole}. \quad (1c)$$

The magnetic susceptibility is therefore nearly uniaxial (accidentally) with large anisotropy in the  $ac$  plane; the principal axis lies in the  $ac$  plane located near the shorter Fe-Cl bonds. From measurements of the temperature dependence of the principal susceptibilities, Narath concluded that an antiferromagnetic ordering transition occurs near 23 K, with the low temperature phase having sublattice spins along the  $\alpha$  axis. Assuming a Curie-Weiss dependence in the paramagnetic region results in Weiss constants

$$\theta_\alpha = +12 \text{ K}, \quad \theta_\beta = \theta_\gamma = +5 \text{ K} \quad (2a)$$

and  $g$  factors

$$g_\alpha = 2.4, \quad g_\beta = g_\gamma = 1.9, \quad (2b)$$

with effective spin  $S=2$ , the free-ion spin.

The symmetry of the magnetic structure was also explored by Narath<sup>12</sup> using proton NMR techniques. At 4 K a close (25 MHz) spin-spin doublet was observed at 9.229 MHz, with no other resonances in the 5.7–25-MHz range. The source of the observed splitting is the dipole field due to the magnetic moments. The single resonance demonstrates that the dipole field is identical at all the proton positions. This is equivalent to requiring that all proton positions be related by magnetic-space-group operations. Since the protons are related by the point group  $C_{2h}$ , the  $\text{Fe}^{2+}$  moments must be invariant under these symmetry operations combined with parity inversion. This can only occur if the moments are parallel to the  $b$  axis or lie in the  $ac$  plane. Tests of the directions of the field at the proton site confirmed that the spins are parallel or antiparallel to the uniaxial  $\alpha$  axis.

The magnetization curve at 4 K for fields along the  $\alpha$  axis shows two steps occurring at values<sup>12</sup>

$$H_{c1} = 39 \pm 1 \text{ kG}, \quad H_{c2} = 46 \pm 1 \text{ kG}. \quad (3)$$

Similar behavior was observed also in CC2 at fields of 35 and 45 kG, respectively.<sup>13,19</sup> Oguchi and Takano<sup>20</sup> initially proposed a four-sublattice model for CC2, whereas Narath<sup>21</sup> concluded that a six-sublattice model was required to explain the magnetization curve. Neutron diffraction studies by Cox *et al.*,<sup>22</sup> and more recently by Weitzel and Schneider<sup>23</sup> confirm the latter model; in the intermediate field region the reflections observed were consistent with a unit cell tripled in the  $a_0$  direction. Schneider and Weitzel<sup>24</sup> have also obtained direct evidence confirming the six-sublattice model for FC2. In addition, they observe a triple point at  $T_T = 11.7 \text{ K}$  and  $H_T = 42.0 \text{ kG}$ , in agreement with the measurements of Lowe *et al.*<sup>25</sup>

Comparing these results with those for CC2 we find that there are some important differences. In FC2 the susceptibility is uniaxial, with the principal direction lying in the  $ac$  plane; in CC2 the susceptibility has a strong transverse anisotropy, and the principal axis is along  $b$ . Consequently, FC2 is best described by the free-ion spin  $S=2$ , while CC2 is fitted best with fictitious  $S=\frac{1}{2}$  and an Ising model. We discuss later how these differences give rise to significantly different excitation spectra.

### C. Optical properties

The optical properties of these materials have been studied by microwave and infrared absorption. Date and Motokawa<sup>26</sup> observed microwave absorption resonances in CC2 and identified them with spin clusters. In an extension of some unpublished work by Silvera,<sup>27</sup> Torrance and Tinkham<sup>14,28</sup> studied the infrared absorption spectrum of CC2 and found metamagnetic phase transitions at  $H_{c1}$  and  $H_{c2}$ , in agreement with earlier studies. In addition to the expected spin excitation with field dependence indicating  $g \approx 7$ , excitations with  $g=14, 21, 28,$  and  $35$  were observed. Their energies were found to be somewhat less than  $n$  times that of the  $g \approx 7$  excitation ( $n = \frac{1}{7}g$ ), and were subsequently identified as bound states of  $n$ -fold spin clusters propagating in the ferromagnetic chain, with spin direction reversed from that of the chain. Using an idealized-linear-chain model which neglects transverse exchange, Torrance and Tinkham<sup>28,29</sup> showed that both the single-spin excitations and  $n$ -fold clusters are allowed eigenstates.

Unlike CC2, which has strong transverse anisotropy, FC2 has uniaxial magnetic symmetry. Consequently, rather than incorporating a spin- $\frac{1}{2}$  formalism and an anisotropic  $g$  factor, the spin Hamiltonian is best expressed as<sup>6</sup>

$$\begin{aligned} H_s = & -g\mu_B H_0 \sum_i S_i^z - D \sum_i [(S_i^z)^2 - \frac{1}{3} S(S+1)] \\ & - \sum_{i,r} J_r \vec{S}_i \cdot \vec{S}_{i+r} - \sum_{i,r} J_r^A S_i^z S_{i+r}^z. \end{aligned} \quad (4)$$

Here  $D$  includes the longitudinal anisotropy,  $J_r$  is the exchange coupling to neighboring spin  $r$ , and  $J_r^A$  expresses the transverse anisotropy. The  $S_i$  and  $S_{i+r}$  are coupled by  $J_r$  and  $J_r^A$ . There are four exchange couplings of interest:  $J_0$  (intra-chain) operates via a Fe-Cl-Fe bond,  $J_1$  via Fe-O-H-Cl-Fe,  $J_2$  via the Fe-Cl-Cl-Fe bond between adjacent chains in the  $ac$  plane, and  $J_3$  via Fe-O-H-H-O-Fe along the  $b$  axis. It is anticipated that

$$|J_0| > |J_1| > |J_2| > |J_3|,$$

with  $|J_2|$  and  $|J_3|$  being quite small. Hay and Torrance<sup>6</sup> have computed the  $k=0$  spin-wave energies and fitted them to infrared absorption data, with results

$$g = 2.23 \pm 0.02, \quad (5a)$$

$$E_0 = 28.75 \pm 0.15 \text{ cm}^{-1}, \quad (5b)$$

$$H_{c1} = 35.0 \pm 0.5 \text{ kG}, \quad (5c)$$

$$H_{c2} = 45.0 \pm 0.5 \text{ kG}, \quad (5d)$$

$$J_1^A/J_1 = J_2^A/J_2 < 0.03, \quad (5e)$$

$$J_1 = -0.27 \text{ cm}^{-1}, \quad (5f)$$

$$J_2 = -0.044 \text{ cm}^{-1}, \quad (5g)$$

$$D = 9.58 \pm 0.05 \text{ cm}^{-1}. \quad (5h)$$

While the absolute value of  $J_0$  is not obtained, the anisotropic part  $J_0^A$  is found<sup>6</sup> to be negligibly small, in agreement with Narath's measurements. The bound-state spin clusters observed in CC2 are not then expected in FC2, since the mechanism for exciting them depends on a large transverse anisotropy<sup>28,29</sup> for sufficient admixture of Ising basis functions so that photon absorption is permitted.

Their spectra show, however, an additional excitation which repels the magnon lines as the magnetic field is varied. This is identified as an optic phonon with energy  $\omega_p = 31.5 \text{ cm}^{-1}$ , made infrared active through a magnon-phonon interaction. A phenomenological calculation<sup>7</sup> gives the coupling constant  $\delta_{AF}^o = 0.92 \text{ cm}^{-1}$  in the antiferromagnetic phase. Torrance and Slonczewski<sup>7</sup> have proposed that this interaction arises from a modulation of the orbital angular momentum by the crystal field at the spin site and a consequent transfer to the spin via spin-orbit coupling. Because of its unusually low frequency, the phonon mode is anticipated to be related to the weak bonds of the waters of hydration; since deuteration shifts the frequency by  $\sim 5\%$ ,<sup>30</sup> these authors expect a rigid motion of the water molecule to dominate. Since the phonon is nominally a  $k=0$  optical infrared inactive mode, it must be of even parity.

For the  $z$  axis parallel to  $b$ , the leading term in the interaction Hamiltonian is

$$H_{\text{int}} = 3\lambda^2 [t_{yz}(S_y S_x + S_z S_y) + t_{xy}(S_x S_y) + t_{xz}(S_x S_z + S_z S_x)] \\ + (1/\Delta_{xy}^2)(t_{xx} - t_{zz})S_y^2 + (1/\Delta_{yz}^2)(t_{yy} - t_{zz})S_x^2, \quad (6)$$

where  $t_{ij}$  is the phonon amplitude,  $\lambda$  is the spin-orbit splitting, and  $\Delta$  is the crystal-fields splitting between the orbital doublet and triplet. Torrance and Slonczewski<sup>7</sup> have shown that the terms  $t_{xz}$  and  $t_{yz}$  couple one phonon to one magnon. Then, the  $|xz\rangle$  and  $|yz\rangle$  phonons with polarizations in the  $ac$  plane are coupled to magnons. The theoretical coupling coefficient they obtain is very near the observed value<sup>6</sup>  $\delta_{AF}^o = 0.94 \text{ cm}^{-1}$ , and it is concluded that in FC2, because covalency effects are small, a point-charge calculation of the interaction gives good results.

## II. PHONON GROUP-THEORETICAL ANALYSIS

Using standard group-theoretical techniques we have determined the number and symmetry of the optical phonon branches at the crystallographic Brillouin-zone center. The result is

$$\Gamma = 6A_g + 6B_g + 5A_u + 7B_u, \quad (7)$$

of which the  $6A_g$  modes are Raman active for  $xx$ ,  $yy$ ,  $zz$ , and  $xy$  polarizability components, and the  $6B_g$  modes are present in the  $xz$  or  $yz$  spectra.

In order to ascertain which of these modes correspond to internal vibrations of the water molecules, we have repeated the calculation, this time treating the water molecules as rigid entities. This yields

$$\Gamma_{\text{lattice}} = 3A_g + 3B_g + 3A_u + 3B_u, \quad (8)$$

which indicates that half of the Raman active modes of each symmetry will correspond to internal water vibrations. We anticipate finding the internal vibrations at relatively high frequencies and the lattice phonons at much lower frequencies ( $< 1000 \text{ cm}^{-1}$ ).

## III. EXPERIMENTAL PROCEDURES

### A. Growth and preparation of crystals

Iron chloride forms three stable hydrates: hexahydrate ( $\text{FeCl}_2 \cdot 6\text{H}_2\text{O}$ ), tetrahydrate ( $\text{FeCl}_2 \cdot 4\text{H}_2\text{O}$ ), and dihydrate ( $\text{FeCl}_2 \cdot 2\text{H}_2\text{O}$ ). The form that precipitates from a saturated solution depends on the ambient temperature. At high temperature all the hydrates decompose to  $\text{FeCl}_2$  and water vapor. The commercially available form is the tetrahydrate, which is stable in the temperature range  $12.3$ – $76.5^\circ\text{C}$ . Above  $76.5^\circ\text{C}$  the stable precipitate from water solution is the dihydrate.<sup>31,32</sup>

Single crystals of FC2 were grown by slow evaporation from a saturated aqueous solution maintained at  $80^\circ\text{C}$ . The crystals are normally in the form of slender prisms, with the long axis parallel to  $[001]$ . The existence of a well developed  $(201)$  face makes it possible to completely deter-

mine the orientation of all crystal axes from the external morphology, and this may be confirmed by examining the crystal under a polarizing microscope.

The FC2 crystals undergo a number of reactions with the atmosphere that make it important to protect the surfaces. In a dry atmosphere the surface emits water, leaving an opaque coating of  $\text{FeCl}_2$ . In a damp atmosphere the crystal is hygroscopic and forms the tetrahydrate. Finally, oxygen in the air can oxidize the iron to  $\text{Fe}^{3+}$ . To preserve the optical quality it was necessary to store the crystals under toluene. For use in the experiment, the samples were coated with a thin layer of inert, transparent coating of dimethyl silicone (for room temperature spectra), or removed from the toluene and immediately immersed in helium gas and cooled to cryogenic temperatures where the surface is stable.

Due to the weak interchain bonds the crystals may be cleaved easily in any plane containing the  $c$  axis, and so excellent (100) and (010) faces were obtained. Good (001) faces were more difficult to obtain, but usable faces were achieved using a wire saw with a solvent consisting of 50% methanol and 50% toluene.

#### B. Apparatus and experimental technique

For the studies of the FC2 phonon spectra and the magnetic field dependence of the magnon-phonon interaction, the sample was directly immersed in liquid helium within a Janis optical tail Dewar. To eliminate light scattering from bubbles in the liquid helium, a vacuum pump was used to lower the helium temperature below the  $\lambda$  point. Magnetic fields to 28 kG were produced by a Varian 15-in.-high homogeneity electromagnet. The Raman studies of the magnon-phonon coupling temperature dependence were made with the sample placed in an Oxford Instruments optical tail Vari-Temp Dewar. The crystal was attached to a copper block containing a thermometer and heater, and mounted in a helium exchange gas atmosphere. With this system the temperature could be controlled to  $\pm 0.05$  K, but because of laser heating effects, the absolute sample temperature was known only to  $\pm 2$  K.

The samples were illuminated with either 488.0- or 514.5-nm light from an argon-ion laser. The scattered light was collimated and directed to the spectrometer entrance slit. A Spex 0.75-m focal length double-grating spectrometer was used. The signal was detected by a thermoelectrically cooled ITT FW130 photomultiplier tube, and the photoelectron pulses were counted electronically. The field-dependence spectra were recorded on a stripchart, while the temperature-dependence spectra were obtained using multiscanning techniques, and the

data were stored in a multichannel analyzer.

### IV. EXPERIMENTAL RESULTS AND ANALYSIS

#### A. Raman spectra

We have observed all the 12 even-parity modes, as tabulated in Table I. For each mode the frequency and symmetry description is given, and in addition we attempt to identify the atomic motion. This latter assignment is fairly accurate for the internal water vibrations, but is only approximate for the lattice vibrations. Beattie *et al.*<sup>33</sup> have performed a similar study for  $\text{CuCl}_2 \cdot 2\text{H}_2\text{O}$ , whose structure is closely related to that of FC2, and the results show a reasonable similarity in all respects.

The lowest-frequency mode is identified as a librational motion of the water molecules. In Fig. 2 we present typical low-frequency spectra for different scattering geometries which show very clearly the  $B_g$ -symmetry nature of the librational mode. The temperature dependence is shown in Fig. 3, and we see that it is in fact "soft," decreasing in energy by about 15% between room temperature and liquid-helium temperature.

Below  $T \approx 23$  K the magnon line appears in the spectrum to the high-energy side of the phonon. Also shown in Fig. 3 is the very small renormalization of the magnon up to the Néel point; near  $T_N$  the magnon line disappears very rapidly with only a slight increase in temperature.

In Figs. 4-9 we show the spectra obtained at 2 K and various applied fields. The dots are data points, and the curve is a least-squares fit to a model described below. Examination of these data shows clearly that there is an interaction between the low-energy excitation (the phonon at zero field) and the upper excitations (antiferromagnetic magnons). With increasing field the lower magnon approaches the phonon, a level repulsion occurs, and eventually a nearly complete reversal of roles occurs. It is also apparent in Fig. 4 that no zero-

TABLE I. Phonons in  $\text{FeCl}_2 \cdot 2\text{H}_2\text{O}$ .

Frequency ( $\text{cm}^{-1}$ )	Symmetry	Type	Bond
36	$B_g$	Libration	$\text{H}_2\text{O}$
148	$A_g$	Distortion	$\text{Cl-Fe-Cl}$
198	$B_g$	Stretch	$\text{Fe-Cl}$
202	$A_g$	Stretch	$\text{Fe-Cl}$
377	$B_g$	Distortion	$\text{O-Fe-Cl}$
500	$A_g$	Stretch	$\text{O-Fe}$
594	$A_g$	Rocking	$\text{O-H}_2$
644	$B_g$	Rocking	$\text{O-H}_2$
1625	$B_g$	Distortion	$\text{H-O-H}$
1800	$A_g$	Distortion	$\text{H-O-H}$
3392	$A_g$	Stretch	$\text{O-H}$
3432	$B_g$	Stretch	$\text{O-H}$

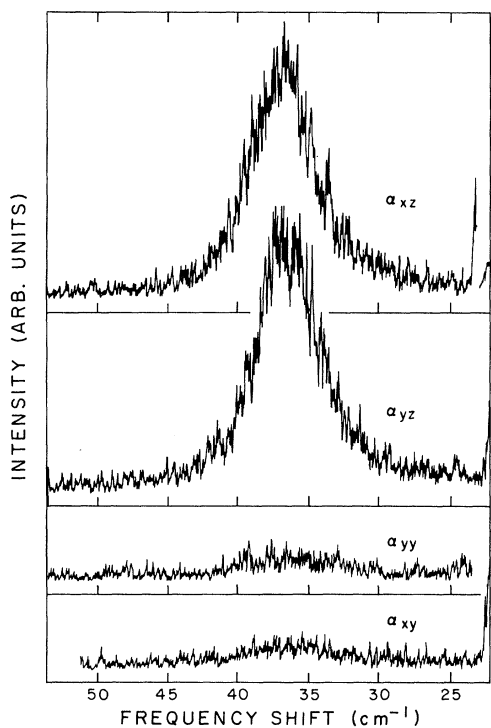


FIG. 2. Spectra of the libration mode showing the  $\alpha_{xx}$  and  $\alpha_{yz}$  polarizabilities expected for  $B_g$  symmetry.

field splitting of the magnon is detected, in disagreement with the  $0.8\text{-cm}^{-1}$  splitting inferred from the infrared data by Hay and Torrance.<sup>6</sup> Finally, we report that there is no evidence in the Raman spectra of spin clusters in the frequency region  $\omega \gtrsim 35\text{ cm}^{-1}$ .

#### B. Analysis

The coupled-mode spectra in Figs. 4–9 may be analyzed mathematically to obtain parameters of

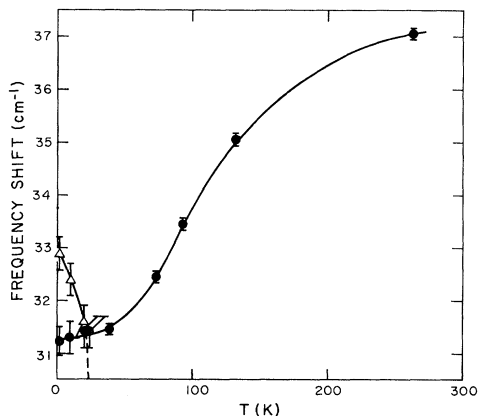


FIG. 3. Frequency vs temperature for the librational phonon (circles) and the magnon (triangles).

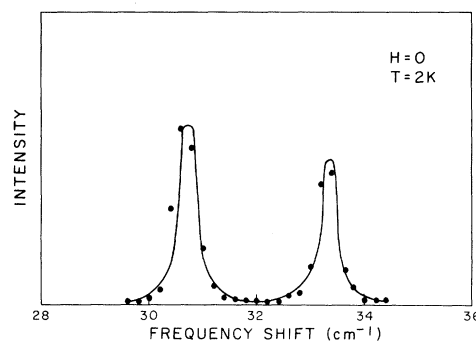


FIG. 4. Phonon-magnon spectrum at  $T=2\text{ K}$  and  $H=0$ . The solid curve is a least-squares fit to Eq. (11).

interest, the uncoupled frequencies, intensities, linewidths, and coupling coefficient. We have made this analysis employing a Green's-function technique which is due to Cowley,<sup>34</sup> and which has proved very successful in studying phonon-phonon interactions.<sup>35</sup>

The Raman intensity scattered into unit solid angle is given by

$$I(\omega) = \frac{\omega_0^4}{2\pi c^3} \sum_{\substack{i,k \\ j,l}} e_i e_k I_{ijkl}(\omega) E_j E_l, \quad (9)$$

where  $\omega_0$  is the laser frequency, the  $e_i$  are polarization vectors of the scattered light, and the  $E_j$  are the incident fields. The scattering coefficient  $I_{ijkl}(\omega)$  is a Fourier-transformed correlation of polarizability operators

$$I_{ijkl}(\omega) = \frac{1}{2\pi} \int_{-\infty}^{+\infty} \langle P_{kl}(t) P_{ij}^\dagger(0) \rangle e^{i\omega t} dt. \quad (10)$$

When these operators are expressed in terms of the normal modes of the crystal, the coefficient becomes for Stokes scattering

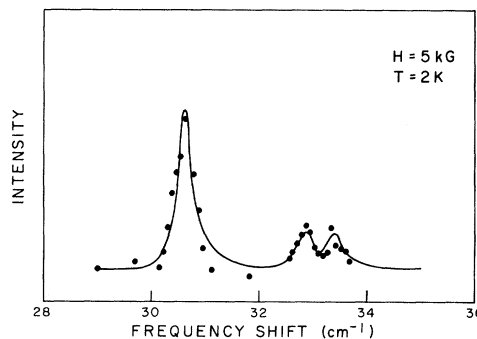


FIG. 5. Phonon-magnon spectrum at  $T=2\text{ K}$  and  $H=5\text{ kG}$ . Note that the observed splitting is  $\sim 1\text{ cm}^{-1}$ , about the same magnitude of the zero-field splitting claimed by Hay and Torrance (Ref. 6).

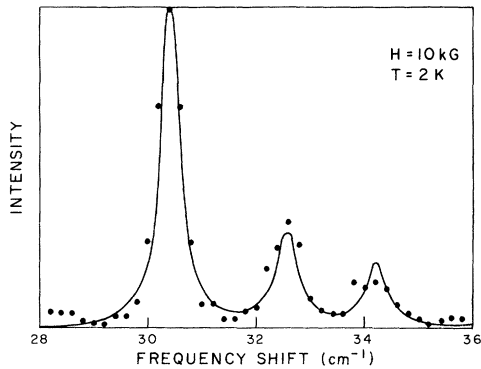


FIG. 6. Phonon-magnon spectrum at  $T=2$  K and  $H=10$  kG.

$$I_{ijkl}(\omega) = [n(\omega) + 1] \sum_{m, m'} P_{ij}(m) P_{kl}(m') \text{Im}[G_{mm'}(\omega)], \quad (11)$$

where  $n(\omega)$  is the Bose population factor, and  $G(\omega)$  is the one-particle Green's function which is directly proportional to the susceptibility.

In the harmonic approximation the excitations are orthogonal and  $G_{mm'}(\omega) (m \neq m') = 0$ ; the response then consists of a series of  $\delta$  functions at the poles of  $G(\omega)$ . Anharmonic interactions, however, give rise to broadening and renormalization of these poles, and the off-diagonal components become non-zero. They become especially important when excitations have very nearly the same energy and wave vector, and then a level repulsion may occur together with line-shape anomalies. In the phonon problem the off-diagonal terms have the general form<sup>36</sup>

$$G_{mm'}(\omega) = 2(\omega_m \omega_{m'})^{1/2} (\delta_{mm'} + i\gamma_{mm'} \omega). \quad (12)$$

They arise from a consideration of the decay of phonons into some final phonon states. In spin-wave formalism there is no direct equivalent of

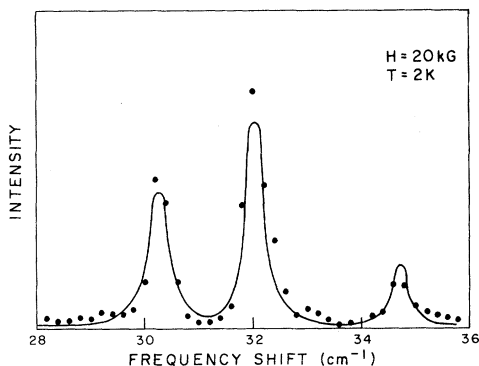


FIG. 7. Phonon-magnon spectrum at  $T=2$  K and  $H=20$  kG.

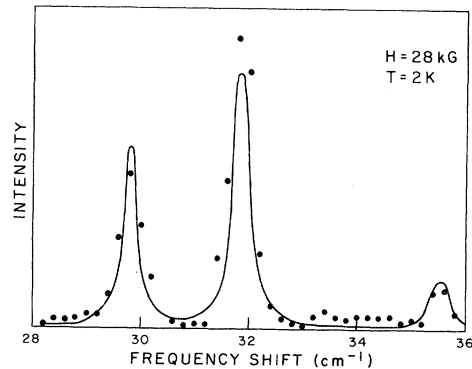


FIG. 8. Phonon-magnon spectrum at  $T=2$  K and  $H=28$  kG.

this. However, if we make the assumption that only the real part of (12) is nonzero, we obtain an expression which describes a level repulsion without any line-shape effects. The coupling constant  $\delta$  can then be compared directly with that obtained in the infrared experiment.<sup>6,7</sup>

The terms  $G_{mm}(\omega)$  describe the uncoupled response of the excitations. The phonon may be adequately described by the familiar damped harmonic oscillator function

$$G_p(\omega) \sim (\omega_p^2 - \omega^2 + i\gamma_p \omega)^{-1}. \quad (13)$$

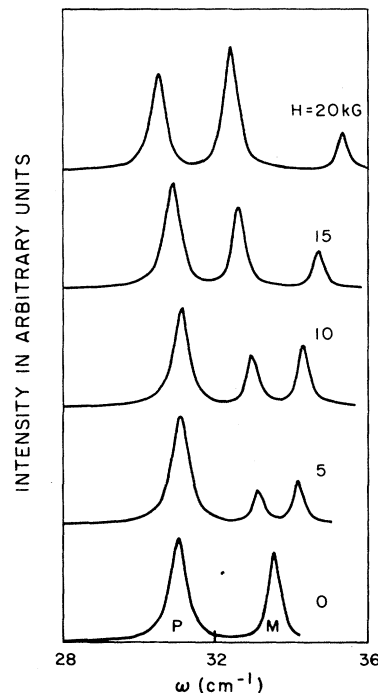


FIG. 9. Superposition of the phonon-magnon spectra at 2 K and various applied fields.

TABLE II. Line-shape analysis of  $\text{FeCl}_2 \cdot 2\text{H}_2\text{O}$  Raman-spectra coupled-mode parameters at  $T=2$  K (units in  $\text{cm}^{-1}$ ) (Subscript 1 refers to phonon parameters, 2 and 3 refer to the magnons.)

	$H$ (kG)				
	0	5	10	20	28
$P_1$	16.45	26.3	61.1	53.2	54.9
$\gamma_1$	0.28	0.31	0.37	0.48	0.3
$\omega_1$	31.2	31.0	31.1	31.2	31.2
$P_2$	4.87 <sup>a</sup>	4.1	6.2	9.4	5.8
$\gamma_2$	0.29	0.42	0.5	0.3	0.3
$\omega_2$	32.9	32.6	32.2	31.4	30.7
$P_3$	4.87 <sup>a</sup>	4.1	6.2	9.4	5.8
$\gamma_3$	0.29	0.42	0.5	0.3	0.3
$\omega_3$	32.9	33.2	34.0	34.5	35.3
$\delta$	0.72 <sup>b</sup>	0.64	0.90	0.86	1.04

<sup>a</sup>The Raman scattering strengths  $P_2$  and  $P_3$  for the *uncoupled*-magnon scattering strengths are about 5 times those quoted for magnons in  $\text{FeF}_2$  (Ref. 43) in absolute intensity. These quoted values represent the most probable values, in a least-squares sense; however, the uncertainty associated with the quoted values is by no means symmetric. It is possible to get a reasonably good fit to the data with the assumption that *all* of the scattering strength in the coupled modes is due to the phonon; i. e.  $P_1 \gg P_2, P_3$ —or  $P_2 = P_3 = 0$ . In other words, the scattering intensities of both magnon- and phonon-like excitations are almost entirely phonon attributable, and the uncoupled-magnon intensity cannot be evaluated accurately.

<sup>b</sup>In the least-squares fit the phonon-magnon coupling constant is strongly correlated with the uncoupled values of phonon and magnon frequency. It consequently is correlated strongly with the magnon  $g$  value, which might explain the discrepancy between the value  $1.7 \pm 0.1$  quoted in the present work and Torrance's value of  $2.23 \pm 0.02$ . Since the present work involves a fitting of *line shape* in addition to the simple separation of peak positions of magnon and phonon, we believe that our evaluation is more accurate and our quoted uncertainties (standard errors of a least-squares fit) more realistic than those of Torrance. In the fits listed in Table II the same starting values were assumed for all parameters at each field value; while this does not eliminate the problem of "trapping down" on a local minimum in the multidimensional least-squares space, it does ensure that the quoted values are self-consistent.

In spin systems the magnon response is quite different; from the modified Bloch equations we find

$$G_m(\omega) \sim \omega_m^{-1} (\omega_m - \omega + i\gamma_m)^{-1}. \quad (14)$$

When  $\omega_m \gg \gamma_m$ , (14) is very nearly Lorentzian. However, when  $\omega_m \approx \gamma_m$  there are some important differences; for example, the observed peak is not displaced from  $\omega_m$  as it is in the Lorentzian. When  $\omega \sim \omega_m$  and  $\omega_m \gg \gamma_m$ , the two response functions are almost indistinguishable, so that the oscillator expression provides a good description of the magnon response.

Finally, we note that in making these approxima-

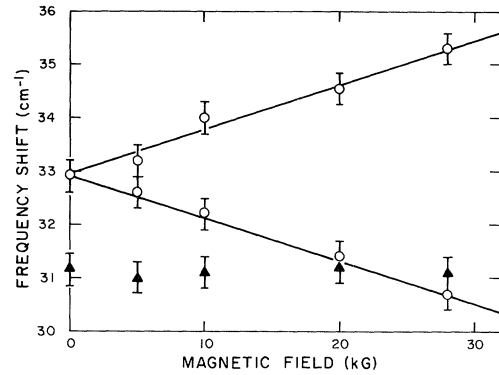


FIG. 10. Uncoupled phonon and magnon frequencies vs field. The splitting for the magnon corresponds to a gyromagnetic ratio (for  $S=2$ ) of  $g=1.7 \pm 0.1$ , which is significantly less than the  $2.23 \pm 0.02$  reported in Ref. 6.

tions we obtain a response function identical to that used by Kobayashi<sup>37</sup> for the pseudospin-phonon interaction in ferroelectric  $\text{KH}_2\text{PO}_4$ .

The values of the parameters obtained by making a least-squares fit to this model are given in Table II. The only constraints made are that the magnon strengths and widths are the same, i. e.,  $P_2 = P_3$ ,  $\gamma_2 = \gamma_3$ . Figure 10 shows the field dependence of the uncoupled magnons and phonon. The splitting corresponds to a  $g$  value of 1.7 for  $S=2$ . This compares well with Narath's<sup>12</sup> value of 1.9, but is somewhat less than Hay and Torrance's<sup>6</sup>  $g=2.23$ . The value of  $\delta$  obtained is also slightly low compared to that measured by Hay and Torrance, and in addition shows a slight field dependence. We

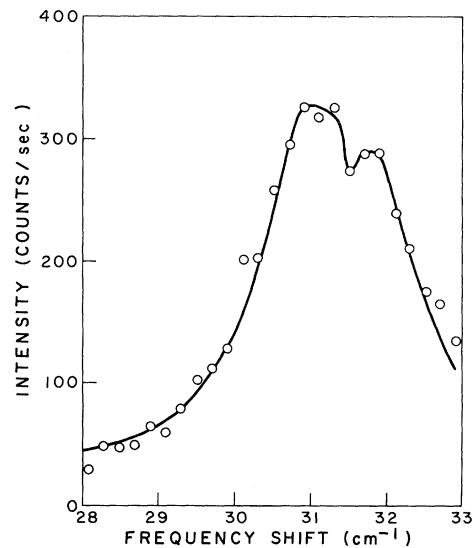


FIG. 11. Phonon-magnon spectrum at  $T=20 \pm 2$  K and  $H=0$ . Solid curve is a least-squares fit to Eq. (11).

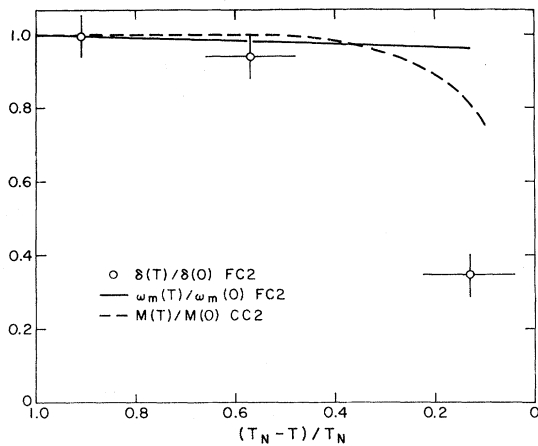


FIG. 12. Phonon-magnon coupling constant vs reduced temperature (open circles). The solid line is the magnon renormalization, which is proportional to  $\kappa$  in Eq. (18). The broken line is the sublattice magnetization in CC2 obtained from proton NMR data. All quantities are normalized to their  $T=0$  K values.

believe that this may reflect some systematic error present in doing a multi-parameter least-squares fit, such as a correlation between  $\delta$  and the other parameters. This may also explain the slightly low  $g$  value obtained. [We believe that the uncertainty in gyromagnetic value quoted by Torrance ( $2.33 \pm 0.02$ ) is somewhat optimistic and does not include the systematic error inherent in the assumption of a (nonexistent) zero-field magnon splitting.]

The temperature dependence of the coupled-mode spectrum has also been studied and analyzed in the manner just described. Figure 11 shows the spectrum at about  $3^\circ\text{C}$  below  $T_N$ . We find that the coupling constant is temperature dependent, and, as shown in Fig. 12, it decreases to zero at  $T \rightarrow T_N$ . We discuss below a simple theory which provides a qualitative description of this result.

## V. DISCUSSION

### A. Magnon renormalization

In the mean-field model of antiferromagnetism the magnon energy is expected to renormalize to zero in a fashion similar to that of the sublattice magnetization. These data are not available for FC2, but the form of the magnetization in CC2 can be obtained from the NMR data. In Fig. 12 the FC2 magnon energy is plotted versus reduced temperature along with  $M(T)$  for CC2 deduced from the proton NMR.<sup>13</sup> It is apparent that in both materials the magnon renormalization with temperature is very slow.

Narath<sup>38</sup> has suggested that this effect may be due to large anisotropy. The anisotropy is large

in both materials ( $\omega_m \sim 30 \text{ cm}^{-1}$ ), and so there is little dispersion throughout the Brillouin zone. Since  $\hbar \omega_m \sim 2k_B T_N$ , very few spin waves are thermally excited until the Néel point is reached. Magnons are then excited throughout the zone, thereby rapidly reducing the sublattice magnetization. Consequently the spin-wave excitation energy decreases rapidly at  $T_N$ .

A second possible explanation, proposed by Silvera *et al.*,<sup>39</sup> invokes a magnetoelastic interaction in which exchange forces responsible for magnetic order are strongly dependent on lattice spacing. At low temperature, where the degree of order is high, the exchange energy will be greater, giving rise to a greater lattice distortion, which in turn causes an increased exchange coupling and so a higher effective  $T_N$ . This mechanism insures that as the temperature rises the magnetization maintains its low temperature value, until at the actual transition point it falls rapidly. In FC2, however, the  $\text{Fe}^{2+}$  ion is in a pure spin state and so may not be strongly coupled to the lattice. On the other hand, the unquenched  $\text{Co}^{2+}$  in CC2 may be sufficiently coupled to make this effect significant. Indeed, a small anomaly in the lattice constants of CC2 is observed at  $T_N$ .<sup>16</sup>

Finally, we briefly consider the one-dimensional nature of FC2 and its relation to the spin-wave spectrum. We know that a linear chain of interacting spins cannot support long-range order for  $T > 0$  (and zero applied field), even when the spin is constrained to one direction. The material TMMC [ $(\text{CD}_3)_4 \text{NMnCl}_3$ ] is a good example. It is a one-dimensional paramagnet for  $T > 1.1$  K, below which it orders antiferromagnetically. Recent neutron-scattering results<sup>40</sup> have shown that spin waves do occur in this system, although only for wavelengths shorter than a characteristic spin correlation length in which spin order exists. It is found both experimentally<sup>40</sup> and theoretically<sup>41</sup> that there is a temperature-dependent broadening but little renormalization of the magnons. McLean and Blume<sup>41</sup> explained this as follows: The order parameter  $\phi$  is defined in terms of the local average magnetization

$$\langle\langle \vec{S}(r, t) \rangle\rangle = \phi \vec{i}(r, t),$$

where  $\vec{i}(r, t)$  is a unit vector giving the direction of the local magnetization. Since the spin-wave renormalization and the local magnetization are directly related, the classical result may be used that  $\phi$  is given by the nearest-neighbor correlation. Thus for the classical linear chain

$$\omega_m \propto \phi \approx 1 - T/2JS(S+1). \quad (15)$$

Consequently, the larger the values of  $J$  and  $S$ , the slower the magnon renormalization.

The situation in FC2, however, is rather differ-



ent; it is not a true one-dimensional system since there is considerable interchain coupling which gives rise to the high ordering temperature. Nevertheless, we expect one-dimensional effects to be manifest to some degree in the ordered phase. Above  $T_N$  there may be sufficient short-range ferromagnetic order along the chains that the above considerations would then apply. However, there is no direct evidence to support this assertion.

While it is difficult to say which of the above mechanisms will dominate, it is fair to say that some combination of them will operate and so give a slow magnon renormalization.

#### B. Temperature dependence of the coupling constant

A qualitative description of the observed temperature-dependent magnon-phonon coupling may be developed from an inspection of the magnon-phonon coupling Hamiltonian, in which the leading term corresponding to single-magnon-single-phonon coupling in FC2

$$\mathcal{H}_{1m-1ph} = \text{const} (S_y S_x + S_x S_y). \quad (16)$$

The constant factor involves crystal-field-state energy differences and a term proportional to the relevant phonon amplitude. We will consider the temperature dependence of the constant to be negligible and assign the total temperature variation of the magnon-phonon interaction to the spin-dependent terms in Eq. (16).

Since the characteristic frequencies of the coupled magnon and phonon are commensurate, the effective temperature behavior of  $\mathcal{H}_{1m-1ph}$  would not be properly reflected in a static thermal average of the spin-dependent term. In other words, the phonon does not respond to a dc average of the spin fluctuations, but, rather, the phonon can follow the spin motion. We approximate this effect by making the *ad hoc* assumption that the effective-temperature-dependent magnon-phonon coupling behaves as

$$\mathcal{H}_{\text{eff}}(T) = \text{const} \langle (S_y^2 S_x^2)^{1/2} \rangle_T. \quad (17)$$

If we evaluate this, and assume that

$$\langle S_x \rangle_T = 2M(T)/M_0,$$

where  $M_0$  is the sublattice magnetization at 0 K, we find

$$\mathcal{H}_{\text{eff}}(T) \sim M(T)/M_0. \quad (18)$$

Figure 12 shows the experimental temperature-dependent magnon-phonon coupling parameter along with a plot of  $\mathcal{H}_{\text{eff}}(T)$  normalized to fit at  $T=0$  K. The temperature dependence of  $M(T)$  is assumed to approximate the temperature variation of the observed magnon frequency at zero applied field. Also shown for comparison is  $M(T)$  for CC2.

It is clear that the simple theory sketched above

is only qualitatively predictive of the observed  $T$  dependence of the phonon-magnon coupling constant. Experimentally, it is found that  $\delta(T)$  decreases faster as  $T \rightarrow T_N$  than the expression in Eq. (18).

#### C. Magnon splitting in zero field

In its antiferromagnetic phase FC2 has space-group symmetry  $P_A 2_1/C$ . Consequently, the two  $k=0$  magnons are nondegenerate and may have different energies. Hay and Torrance<sup>6</sup> and Torrance and Slonczewski<sup>7</sup> have argued that when the magnon-phonon interaction is included this energy splitting is  $\sim 0.8 \text{ cm}^{-1}$ . The Raman data presented here are in contradiction with this conclusion. The spectrum in Fig. 4 shows no evidence of any splitting, and even with  $H=5$  kG the energy difference is only  $\approx 0.6 \text{ cm}^{-1}$ . Torrance (private communication) has argued that only one of the spin waves is Raman active at zero field, and that the other becomes active only for  $H \neq 0$ . Our low-field measurements do not appear to substantiate this. We feel that the published infrared data are inconclusive in this respect, since the zero-field trace shows little evidence of splitting.

The situation in CC2 is quite different, and a real splitting occurs—but not because of coupling to the phonon. Owing to the large transverse anisotropy, there may be coupling<sup>28,29</sup> between spin states with  $\Delta m = \pm 2$ , so that “spin up” and “spin down” magnons will have different energies. The observed splitting is relatively large,  $\sim 4 \text{ cm}^{-1}$ .

#### D. Two-magnon excitation

An unusual feature of the observed spectra is the absence of a two-magnon excitation. In both two- and three-dimensional antiferromagnetic systems Raman scattering by two magnons is found<sup>42</sup> to have intensity greater than that of the single-magnon scattering. This has been explained in terms of different scattering mechanisms for the two processes.<sup>43</sup> First-order scattering is thought to occur indirectly via a spin-orbit coupling of the light electric vector to the spin of the magnetic ion. Higher order terms in this interaction may give rise to multimagnon scattering, but the predicted intensity is very small. However, an exchange scattering mechanism, in which two magnons are created in close proximity in real space, has been able to explain most of the observed features of the two-magnon scattering, including the symmetry and the large intensity. The question which arises here is whether or not the same mechanism operates in linear-chain systems.

In some recent work Lo and Halley<sup>44</sup> have shown that the two-magnon Raman-scattering cross-section for TMMC is zero. The interaction Hamiltonian which describes the process commutes with the crystal Hamiltonian, so that no scattering will

occur. They comment that this result seems to hold for all linear Heisenberg antiferromagnets.

As we have discussed above, FC2 is not a true one-dimensional system. However, we may conclude that because of its accidentally zero transverse anisotropy there is little coupling between spin waves created near each other on the different sublattices, so that the magnitude of the exchange scattering is small.

It is of interest here to remark on the observation of spin clusters observed in CC2 and CB2. Elliott and Thorpe<sup>45</sup> have commented that the same exchange scattering mechanism responsible for two-magnon excitation will give rise to bound pairs.

Torrance and Tinkham have shown in detail how the large transverse anisotropy is directly responsible for the mixing of the magnon basis functions which permits the observation of clusters. This indicates that these two materials are perhaps more suited to the study of two-magnons by Raman scattering.

#### ACKNOWLEDGMENTS

We wish to acknowledge many helpful discussions with D. Nicoli and J. B. Torrance, Jr., and the technical assistance of D. J. Toms in obtaining some of the data.

†Work supported by NSF grant GH-34681.

\*Permanent address: IBM Corporation, Boulder, Colorado.

‡Present address: Clarendon Laboratory, University of Oxford, Oxford, England.

<sup>1</sup>S. J. Allen and H. J. Guggenheim, Phys. Rev. Lett. **21**, 1807 (1968); Phys. Rev. **166**, 530 (1968).

<sup>2</sup>R. A. Cowley and G. Dolling, Phys. Rev. **167**, 464 (1968).

<sup>3</sup>T. M. Holden *et al.*, J. Phys. C **4**, 2127 (1971).

<sup>4</sup>W. J. L. Buyers *et al.*, J. Phys. C **4**, 2139 (1971).

<sup>5</sup>J. B. Torrance, Jr., Ph.D. thesis (Harvard University, 1968) (unpublished).

<sup>6</sup>K. A. Hay and J. B. Torrance, Jr., Phys. Rev. B **2**, 746 (1970).

<sup>7</sup>J. B. Torrance and J. C. Slonczewski, Phys. Rev. B **5**, 4648 (1972).

<sup>8</sup>R. M. MacFarlane and H. Morawitz, Phys. Rev. Lett. **27**, 15 (1971).

<sup>9</sup>P. Moch and C. Dugautier, Phys. Lett. A **43**, 169 (1973).

<sup>10</sup>S. W. Lovesey, J. Phys. C **5**, 2769 (1972).

<sup>11</sup>R. W. Kinne, J. F. Ryan, W. J. O'Sullivan, and J. F. Scott, AIP Conf. Proc. **18**, 390 (1974).

<sup>12</sup>A. Narath, Phys. Rev. **139**, A1221 (1965).

<sup>13</sup>A. Narath, Phys. Rev. **136**, A766 (1965).

<sup>14</sup>J. B. Torrance, Jr. and M. Tinkham, J. Appl. Phys. **39**, 822 (1968).

<sup>15</sup>B. Morosin and E. J. Graeber, Acta Crystallogr. **16**, 1176 (1963).

<sup>16</sup>B. Morosin and E. J. Graeber, J. Chem. Phys. **42**, 898 (1965).

<sup>17</sup>B. Morosin, Acta Crystallogr. **23**, 630 (1967).

<sup>18</sup>A. Abragam and M. H. L. Pryce, Proc. R. Soc. A **205**, 135 (1951).

<sup>19</sup>H. Kobayashi and T. Haseda, J. Phys. Soc. Jpn. **19**, 765 (1964).

<sup>20</sup>T. Oguchi and F. Takano, J. Phys. Soc. Jpn. **19**, 1265 (1964).

<sup>21</sup>A. Narath, Phys. Lett. **13**, 12 (1964).

<sup>22</sup>D. E. Cox, G. Shirane, B. C. Frazer, and A. Narath, J. Appl. Phys. **37**, 1126 (1966).

<sup>23</sup>H. Weitzel and W. Schneider, Solid State Commun. **14**, 1025 (1974).

<sup>24</sup>W. Scheider and H. Weitzel, Solid State Commun. **13**, 303 (1973).

<sup>25</sup>M. A. Lowe, C. R. Abeledo, and A. A. Missetich, AIP Conf. Proc. **5**, 307 (1972).

<sup>26</sup>M. Date and M. Motokawa, Phys. Rev. Lett. **16**, 1111 (1966); J. Phys. Soc. Jpn. **24**, 41 (1968).

<sup>27</sup>I. F. Silvera, Ph.D. thesis (University of California, Berkeley, 1965) (unpublished).

<sup>28</sup>J. B. Torrance, Jr. and M. Tinkham, Phys. Rev. **187**, 587 (1969).

<sup>29</sup>D. Nicoli and M. Tinkham (private communication), cited in Ref. 7.

<sup>30</sup>W. F. Link, *Solubilities of Inorganic and Metal-Organic Compounds* (American Chemical Society, Washington, D. C., 1958), Vol. 1, p. 1013.

<sup>31</sup>V. F. Schimmel, Z. Anorg. Allg. Chem. **176**, 285 (1928).

<sup>32</sup>I. R. Beattie, T. R. Gibson, and G. A. Ozin, J. Chem. Soc. A **1968**, 534 (1968).

<sup>33</sup>R. A. Cowley, *Raman Effect*, edited by A. Anderson (Dekker, New York, 1971), Vol. I; A. Zawadowski and J. Ruvalds Phys. Rev. Lett. **24**, 1111 (1970); Phys. Rev. B **2**, 1172 (1970); A. A. Maradudin and A. E. Fein, Phys. Rev. **128**, 2589 (1962).

<sup>34</sup>J. F. Ryan and K. Hisano, J. Phys. C **6**, 566 (1973); J. F. Scott, Phys. Rev. Lett. **24**, 1107 (1970); R. S. Katiyar, J. F. Ryan, and J. F. Scott, Phys. Rev. B **4**, 2635 (1971).

<sup>35</sup>R. A. Cowley, *Phonons in Perfect Lattices and Lattices with Point Defects*, edited by R. W. H. Stevenson (Plenum, New York, 1966).

<sup>36</sup>K. Kobayashi, J. Phys. Soc. Jpn. **24**, 497 (1968).

<sup>37</sup>A. Narath (private communication), cited in Ref. 39.

<sup>38</sup>I. F. Silvera, J. H. M. Thomley, and M. Tinkham, Phys. Rev. **136**, A695 (1964).

<sup>39</sup>M. T. Hutchings, G. Shirane, R. J. Birgeneau, and S. L. Holt, Phys. Rev. B **5**, 1999 (1972).

<sup>40</sup>F. B. McLean and M. Blume, Phys. Rev. B **7**, 1149 (1973).

<sup>41</sup>P. A. Fleury, Int. J. Magn. **1**, 75 (1970).

<sup>42</sup>P. A. Fleury and R. Loudon, Phys. Rev. **166**, 514 (1968).

<sup>43</sup>S. K. Lo and J. W. Halley, Phys. Rev. B **8**, 5272 (1973).

<sup>44</sup>R. J. Elliott and M. F. Thorpe, J. Phys. C **2**, 1630 (1969).